Diode laser spectroscopy of the ethylene ν_7 band in the region of 960–1030 cm^{-1}

Ya.Ya. Ponurovskii and E.V. Stepanov

Institute of General Physics, Russian Academy of Sciences, Moscow

Received May 6, 2002

More than 200 absorption lines of the C_2H_4 molecule have been recorded in the spectral region from 930 to 1030 cm^{-1} with an automated diode laser spectrometer. More than 60 lines belonging to the ethylene ν_7 band of *C*-type were measured and assigned with the absolute accuracy better than 0.0003 cm^{-1}. Intensities of more than 20 ethylene absorption lines belonging to the studied ν_7 band were accurately determined. These data were used for precise determination of the ethylene transition moment constant $\delta\mu_\chi/\delta q_7$ that was found to be 0.23±0.02 D. This value was then used to calculate of the whole spectrum of the ν_7 band.

Introduction

The knowledge of high-resolution absorption spectra of ethylene (C_2H_4) is urgent in both basic and applied molecular spectroscopy. From the viewpoint of theoretical spectroscopy, this substance is interesting, because it is a rather simple molecule having several close vibrational energy levels strongly interacting due to molecular rotation. The latter circumstance explains significant changes in wavenumbers and intensities of the rotational-vibrational transitions. Therefore, to accurately describe and calculate spectral characteristics of this molecule and similar molecules, specialized methods should be developed.

From the viewpoint of applied studies, it is important to accumulate precision experimental data on the parameters of ethylene absorption lines. This is needed both in compiling high-resolution databases such as HITRAN and GEISA[1–3] and for solution of problems in gas analysis by the methods of molecular spectroscopy. In particular, it is an urgent problem now to develop high-sensitivity methods for laser analysis of C_2H_4 in order to solve various problems in ecology, plant biology, and medicine, because ethylene plays a considerable role in vital activity of living microorganisms as a biomarker and signal molecule.[4]

For the first time, the fine structure of infrared absorption spectra of ethylene in the region of 10 μm was analyzed by Smith and Mills in Ref. 5. Using a diffraction spectrometer having spectral resolution about 0.2 cm^{-1}, they have recorded the C_2H_4 absorption spectra in the region of 700–1100 cm^{-1}. In the process of analysis and assigning the experimental data, they noticed strong Coriolis interaction between energy levels of the ν_4, ν_7, and ν_{10} bands lying in this spectral region. This interaction leads to the significant shifts of rotational-vibrational lines. Lambeau with co-authors[6] have analyzed these levels based on the data of the classical IR spectroscopy,[7] diode laser spectroscopy (DLS),[8] and spectroscopic data obtained using a waveguide CO_2 laser.[9] Solution of the inverse spectroscopic problem allowed determination of the rotational-vibrational energy levels of the ν_4, ν_7, and ν_{10} bands. They have refined the centrifugal distortion constants up to the sixth order inclusive and the Coriolis interaction constants up to the second order.

The most thorough investigations into the ethylene spectroscopy in the region of 10 μm are presented in Ref. 10. Analysis of the ν_4, ν_7, ν_{10}, and ν_{12} bands was based on the extensive FTIR and DLS data. More than 12000 C_2H_4 lines in the region of 800–1090 cm^{-1} were recorded with a Fourier Transform IR (FTIR) spectrometer with the relative accuracy in line positions better than 0.0002 cm^{-1}. To achieve such accuracy, the spectra were calibrated with a waveguide CO_2 laser,[9,11] as well as using 50 well-known C_2H_4 lines taken as reference ones. In addition to the FTIR spectra, more than 2000 ethylene absorption lines in the region of 833–883 cm^{-1} were recorded with a diode laser spectrometer. The absolute frequency calibration was conducted against OCS lines with the accuracy of 0.001 cm^{-1}.

The interest in the DLS data was explained by the presence of weak rotational-vibrational lines belonging to the ν_7 and ν_{10} bands in the spectrum. To process this extensive high-accuracy experimental material, Cauuet et al.[10] used the model accounting for the Watson's Hamiltonian up too the sextic centrifugal distortion constants and additionally included the third order of Coriolis interaction between the rotational levels of the ν_7, ν_{10}, and ν_4 bands.[12] The discrepancies between the calculated and experimental line positions varied from 10^{-4} to 10^{-3} cm^{-1} for different vibrational energy levels and for large values of the angular momentum quantum number J (up to $J = 50$).

In this paper, we present analysis of the ethylene absorption spectra recorded in the region of 960–1030 cm^{-1} with tunable diode lasers (TDL). The information obtained on line positions and absolute intensities complementing the literature FTIR data is used to refine the C_2H_4 spectroscopic and molecular constants.

0235-6880/02/09 766-05 $02.00

1. Experimental setup

In this work, we used a TDL spectrometer, whose design was described earlier (see, for example, Ref. 13). As a tunable source of IR radiation, we employed a diffuse $Pb_xS_{1-x}Se$ TDL operated in a repetitively pulsed mode at the helium temperature from 20 to 80 K. The pulse duration was 8 ms, and the pulse repetition frequency was ~ 100 Hz. The optical layout of the spectrometer included two receiving channels for the TDL radiation coming from two opposite crystal faces. One of the channels was used to record transmission spectra of gaseous molecules under study. It included an analytical cell with a pressure measurement system, a cell with the reference gas, a Fabry–Perot etalon, and a diffraction grating to separate a spectral mode of the radiation. The second channel was used for fine stabilization of the laser frequency against absorption lines of reference gases.

To record signals in each channel, we used cooled CdHgTe photodetectors having the operating speed ~ 20 ns. The signal to be detected was amplified with a broadband pre-amplifier having the pass band of 0–5 MHz. The signal in the measuring channel was entered into a CAMAC computer-controlled digital recording system based on a fast F4226 12-bit ADC with the time resolution of 50 ns. The signal in the reference channel after pre-amplification and, whenever necessary, differentiation came to the system of the diode laser tuning curve stabilization.

Heating the p–n junction of the laser crystal during the pump pulse of electric current, made fine-tuning of the laser frequency used for recording the molecular absorption spectra. The continuous frequency tuning zone in some modes was 2–3 cm^{-1}. The frequency tuning rate during a pulse varied from ~ $3\cdot 10^3$ cm^{-1}/s at the leading edge to ~ 10^3 cm^{-1}/s at the trailing edge. With the used length of the recorded data array (1024 points), this allowed recording of transmission spectra in laser modes by small fragments each about 0.3 to 0.5 cm^{-1} long. In this case, the spectrum length on the time scale was 150–300 μs. With the scanning rates used, the discreteness of the digital spectrum recording ≥ 50 ns provided for the spectral resolution up to 0.00025 cm^{-1}.

Besides the digitization limits, the spectrometer resolution was determined by a number of factors, namely, the laser line width, instability of laser temperature and pumping pulse parameters, high rate of frequency tuning in the repetitively pulsed mode of spectrum recording, as well as the instrumental function of the recording system. High stability of the laser diode temperature was provided by use of two control loops. Electronic stabilization of the cold finger of a cryostat housing of the laser provided for its long-term stability at the level of 0.001 K that corresponded to the lasing frequency stability ~ 0.001 cm^{-1}. Sweep stabilization of the laser frequency scale with respect to the absorption line in the reference channel allowed further decrease of temperature derating of the laser frequency, and thus the reproducibility ~ 0.0002 cm^{-1} was achieved.

The signal-to-noise ratio of laser signal recording was higher than 10^3, and the noise level was determined by the parameters of the recording system, first of all, by the noise of the broadband pre-amplifier, which could be decreased through signal accumulation. The ratio between the levels of the luminescent and laser components of the TDL radiation at the working temperatures was no larger than 2%.

The spectrometer frequency scale was calibrated relative to the transmission spectra of the germanium Fabry–Perot etalon, whose free spectral range, in the region studied, was ~ 0.0482 cm^{-1}. The accuracy of the frequency scale calibration against the etalon was no worse than 0.0005 cm^{-1}. The transmission spectrum of the Fabry–Perot etalon was also used, whenever necessary, for the program linearization of the frequency scale of the studied spectra. To improve the accuracy of the frequency scale reference, we used additional calibration against NH_3 and CO_2 lines[14] (the accuracy in NH_3 line positions is no worse than 0.0003 cm^{-1}) lying in the studied spectral region. As a result, the reference accuracy was improved to ~ 0.0003 cm^{-1}.

For our investigations, we used a standard C_2H_4 gas sample corresponding to GSO 4179-87. The molar fraction of ethylene in the sample was ~ 99.95%. For recording the C_2H_4 absorption spectra, we used a 2-m long cell. The gas pressure was measured with a 6MDX5C mechanotron (pressure measurement range from 0 to 10 Torr, error ~ 8%). When studying C_2H_4 line positions, we maintained the pressure at the level of ~ 0.75 Torr; this allowed polymerization to be avoided and frequencies of the Doppler broadened absorption lines to be measured.

Figure 1 depicts typical experimental absorption spectra of ethylene and ammonia. Their frequency scale was program-linearized with the use of the transmission spectrum of the Fabry–Perot etalon (bottom panel of Fig. 1).

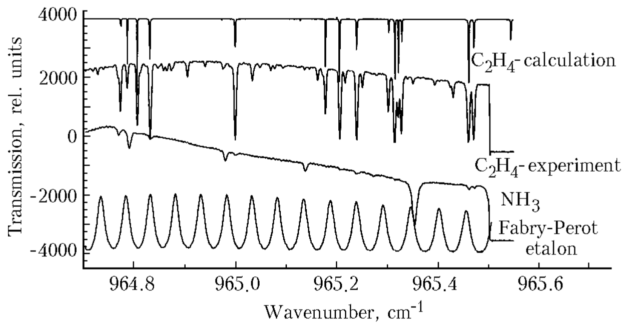

Fig. 1. Transmission spectra of cells filled with ethylene, reference NH_3 gas, and a Fabry–Perot interferometer obtained with a tunable diode laser radiation.

The top panel of Fig. 1 shows the ethylene transmission spectrum calculated based on the results of this study.

2. Results. Analysis and discussion

2.1. Energy levels

The C_2H_4 molecule belonging to the D_{2h} symmetry group is characterized by a specific type of interaction between vibrational energy levels determining the C_2H_4 absorption activity in the region of 10 μm. This interaction of energy levels in ethylene is caused by the Coriolis resonance arising due to the relation between the total angular momentum P_a and the vibrational angular momentum p_a of the molecule. If the product of the symmetry types $\Gamma(g_s)$ of two vibrational modes includes the rotational symmetry type, that is,

$$\Gamma(g_s)\Gamma(g_{s'}) \supset \Gamma(r_a),$$

then the Coriolis interaction occurs between the $(\upsilon_\sigma, \upsilon_{\sigma'})$ and $(\upsilon_\sigma + 1, \upsilon_{\sigma'} - 1)$ states.

Figure 2 depicts the ethylene vibrational energy levels lying between 800 and 1500 cm^{-1} and taking part in the formation of the fundamental ν_4, ν_7, ν_{10}, and ν_{12} bands. This figure also shows the classification of levels by the symmetry types of the D_{2h} group and the type of absorption bands formed by transitions from the ground state υ_0. The dashed lines show the interactions between the levels due to the Coriolis resonance.

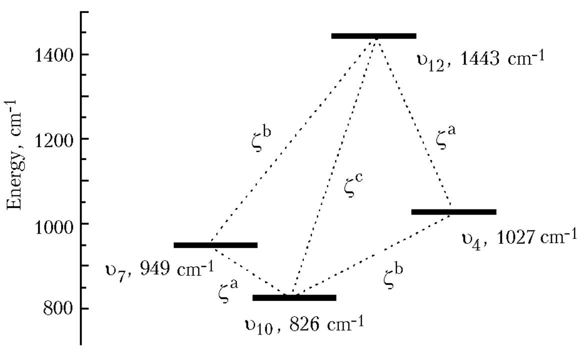

B_{1u}	B_{2u}	B_{3u}	A_u
ν_7	ν_{10}	ν_{12}	ν_4
C	*B*	*A*	IR inactive

Fig. 2. Ethylene vibrational energy levels lying between 800 and 1500 cm^{-1}, their classification by symmetry types of the D_{2h} group, and types of absorption bands formed by transitions to these levels from the ground state υ_0.

The vibrational state υ_7 interacts due to the *A*-type Coriolis resonance with the state υ_{10}, which, in its turn, is connected with the υ_4 state inactive in the IR due to the *B*-type Coriolis resonance. Besides, according to Ref. 15, υ_{12} state is connected with the states υ_7 and υ_4 by the Coriolis resonances with the coefficients $\zeta^{b}_{7,12} = 0.85$ cm^{-1} and $\zeta^{a}_{4,12} = 0.53$ cm^{-1}, respectively. Because of these interactions, the states υ_7 and υ_4 turn out to be related indirectly through resonances with the states υ_{10} and υ_{12}, in spite of the symmetry-forbidden Coriolis resonance between υ_7 and υ_4 states. Thus, υ_4, υ_7, υ_{10}, and υ_{12} form an isolated tetrad of interacting states. The complete Hamiltonian of this system is a sum of the isolated-state Hamiltonians and those of the Coriolis interactions between the states. Accurate to the terms of the sixth order of smallness, the Hamiltonian of an isolated state can be presented as:

$$\hat{H}_{vv}(E+/-, O+/-) = E_v + \{A_n - 1/2(B_v + C_v)\}\,\hat{J}_z + $$
$$+ 1/2\,\{B_v + C_v\hat{J}^2 + 1/2\,(B_v - C_v)\,\hat{J}^2_{xy} - \Delta_K\upsilon\hat{J}^4_z - $$
$$- \Delta_{JK}\upsilon\hat{J}^2_z\,\hat{J}^2 - \Delta_J\upsilon(\hat{J}^2)^2 - \delta_K\upsilon(\hat{J}^2_z\,\hat{J}^2_{xy} + \hat{J}^2_{xy} + \hat{J}^2_{xy}\hat{J}^2_z) - $$
$$- 2\delta_J\upsilon\hat{J}^2_{xy}\hat{J}^2 + H_K\upsilon\hat{J}^6_z + H_{KJ}\upsilon\hat{J}^4_z\hat{J}^2 + H_{JK}\upsilon\hat{J}^2_z(\hat{J}^2)^2 + $$
$$+ H_J\upsilon(\hat{J}^2)^3 + h_K\upsilon(\hat{J}^4_z\,\hat{J}^2_{xy} + \hat{J}^2_{xy}(\hat{J}^2)^2 + h_{JK}\upsilon\hat{J}^2_z\hat{J}^2_{xy} + $$
$$+ \hat{J}^2_{xy}\hat{J}^2_z\}\hat{J}^2 + 2h_J\upsilon\hat{J}^2_{xy}\,(\hat{J}^2)^2\,.$$

The coefficients at the operators $\hat{J}^2$, $\hat{J}_z$, $\hat{J}_{xy}$ are the well known spectroscopic constants of the reduced Watson's Hamiltonian.[16] Accurate to the terms of the third order of smallness, the Hamiltonian of the Coriolis interaction between the levels, for example, for the *x*-type interaction can be written as[12]:

$$\hat{H}_{cor} = i\xi_x\hat{J} + \eta^{yz}_{12}(\hat{J}_y\hat{J}_z + \hat{J}_z\hat{J}_y) + \tau^{yyyz}_{12}(\hat{J}^3_y\,\hat{J}_z + \hat{J}_z\hat{J}^3_y) + $$
$$+ \tau^{yzzz}_{12}(\hat{J}_y\hat{J}^3_z + \hat{J}^3_z\hat{J}_y) + \tau^{xxyz}_{12}(\hat{J}^3_x\hat{J}_y\hat{J}_y + \hat{J}_z\hat{J}_y\hat{J}^3_x),$$

where ξ, η, τ are the parameters of the Coriolis interaction between the levels 1 and 2; $\hat{J}_x$, $\hat{J}_y$, and $\hat{J}_z$ are the operators of projection of the total angular momentum on the axes in the molecular coordinate system. For a given value of the quantum angular momentum J, the energy matrix has the dimension $4(2J+1)$. In the Wang basis,[9] this matrix is divided into four submatrices, each having the dimension of $2J$.

	B_{2u}	B_{1u}	A_u	B_{3u}
υ_{10}	$E^{+/-}$	Cor *Z*	Cor *X*	Cor *Y*
υ_7		$E^{-/+}$	Cor *Y*	Cor *X*
υ_4			$O^{+/-}$	Cor *Z*
υ_{12}				$O^{-/+}$

	B_{2u}	B_{1u}	A_u	B_{3u}
υ_{10}	$O^{+/-}$	Cor *Z*	Cor *X*	Cor *Y*
υ_7		$O^{-/+}$	Cor *Y*	Cor *X*
υ_4			$E^{+/-}$	Cor *Z*
υ_{12}				$E^{-/+}$

Fig. 3. Structure of energy submatrices.

Figure 3 shows the structure of these blocks and the types of Wang submatrices interacting with each other according to different selection rules for Coriolis resonances. To obtain the energy levels and wave functions of the states of interest, these submatrices were diagonalized using the spectroscopic parameters of the Watson's Hamiltonian and the parameters of the Coriolis interaction of the C_2H_4 states studied from Ref. 10.

Table 1 presents calculated values of the rotational-vibrational energy levels with $J = 30$ for the υ_7 state and the mixing coefficient for them that show the degree of relation between the wave functions of different vibrational states.

It can be seen from Table 1 that as K_a increases, the degree of mixing (relation) of rotational states in the tetrad of interacting states increases because of the so-called global Coriolis resonance. Besides, as can be seen from Table 1, there exist local Coriolis resonances as well (for example, for K_a = 4–6).

Table 1. Ethylene rotational-vibrational energy levels with $J = 30$ for the υ_7 state and mixing coefficients

J	K_a	K_c	$E(\upsilon_7)$	$C(\upsilon_{10})$, %	$C(\upsilon_7)$, %	$C(\upsilon_4)$, %	$C(\upsilon_{12})$, %
30	0	30	1743.8274	0.9	98.9	0.0	0.1
30	1	30	1743.8199	0.8	99.1	0.0	0.1
30	1	29	1789.6568	1.4	98.2	0.1	0.3
30	2	29	1789.7299	1.4	98.3	0.1	0.3
30	2	28	1829.2323	1.8	96.7	1.0	0.5
30	3	28	1830.6264	1.8	96.9	0.8	0.5
30	3	27	1858.6546	30.7	65.8	3.1	0.5
30	4	27	1866.1352	0.8	52.4	46.6	0.2
30	4	26	1880.0350	1.2	97.5	0.5	0.8
30	5	26	1904.4834	1.8	85.6	12.1	0.5
30	5	25	1907.8225	2.3	96.4	0.7	0.7
30	6	25	1949.0020	4.6	86.4	8.4	0.6
30	6	24	1948.6907	3.6	94.5	1.3	0.6
30	7	24	1999.7887	5.0	91.6	2.9	0.5
30	7	23	1999.7515	4.9	91.6	3.0	0.5
30	8	23	2059.1835	8.2	81.4	10.1	0.3
30	8	22	2059.1752	8.2	81.3	10.1	0.3
30	9	22	2123.9472	5.5	60.6	33.8	0.1
30	9	21	2123.9459	5.5	60.6	33.8	0.1
30	10	21	2207.4619	14.6	67.7	16.7	1.0
30	10	20	2207.4619	14.6	67.7	16.7	1.0
30	11	19	2291.3437	12.4	80.5	6.2	0.9
30	12	18	2383.6479	13.0	83.0	3.3	0.8
30	13	17	2484.0384	14.0	83.2	2.1	0.7
30	14	17	2592.3762	15.2	82.6	1.5	0.7
30	15	15	2708.5806	16.4	81.8	1.2	0.6
30	16	14	2832.5916	17.6	80.8	1.0	0.6
30	17	13	2964.3576	18.8	79.7	0.9	0.6
30	18	12	3103.8312	20.0	78.7	0.8	0.6
30	19	12	3250.9671	21.2	77.6	0.7	0.5
30	20	11	3405.7211	22.4	76.5	0.6	0.5
30	21	10	3568.0481	23.5	75.4	0.6	0.5
30	22	9	3737.9168	24.7	74.3	0.5	0.5
30	23	7	3915.2646	25.8	73.3	0.5	0.4
30	24	7	4100.0609	27.0	72.2	0.4	0.4
30	25	5	4292.2261	28.1	71.2	0.4	0.4
30	26	5	4491.8232	29.2	70.2	0.3	0.3
30	27	4	4698.7045	30.3	69.2	0.2	0.3
30	28	3	4912.8633	31.4	68.2	0.2	0.2
30	29	2	5134.2583	32.5	67.2	0.1	0.2
30	30	1	5362.8487	33.7	66.2	0.0	0.1

2.2. Experimental results

In spectroscopic investigations in the regions of 964–1975 and 1030–1034 cm^{-1}, we have recorded more than 200 ethylene lines belonging largely to the *Q*- and *P*-branches of the ν_7 band of *C*-type. Some lines belong to the $^{12}C^{13}CH_4$ isotopic modification and the so-called forbidden transitions of the ν_4 band inactive in the IR. We studied the parameters of absorption lines only for the ν_7 band centered near 949 cm^{-1}, because they are several orders of magnitude stronger than the lines of the ν_{10} band (826 cm^{-1}; *B*-type) and ν_{12} band (1443 cm^{-1}; *A*-type) lying in the same spectral region (see Fig. 2). Table 2 (column 2) presents the experimental data on the positions of the strongest lines of the ν_7 band. Column 3 gives the absolute difference between the calculated and experimental wavenumbers of the studied transitions. A close agreement between these data indicates the correctness of our model used for calculations. The largest discrepancy (from ~10^{-4} to ~$5\cdot10^{-4}$ cm^{-1}) between the calculated and experimental line positions is observed for K_a = 6 and 7, where the local Coriolis resonance is the strongest, and for high J.

Table 2. Wavenumbers and intensities of rotational-vibrational transitions of the ν_7 band of ethylene as recorded with the diode laser spectrometer

J	K_a	K_c	J	$K_{a'}$	$K_{c'}$	σ_{exp}, cm^{-1}	$\sigma_{exp}-\sigma_{cal}$, cm^{-1}	$S\cdot10^{20}$, cm·mol^{-1} exp.	calc.
21	7	14	22	6	16	964.7724	−0.0004	0.178+/−0.03	0.168
21	7	15	22	6	17	964.7857	0.0003	0.077+/−0.01	0.072
25	1	24	24	2	22	964.8062	0.0000	0.278+/−0.02	0.299
2	2	0	1	1	0	964.8308	−0.0001	0.795+/−0.02	0.855
2	2	1	1	1	1	964.9990	−0.0002	0.898+/−0.05	0.839
24	1	23	23	2	21	965.1777	−0.0002	0.149+/−0.02	0.161
17	2	15	16	3	13	965.2060	0.0001	0.742+/−0.04	0.694
16	1	15	15	2	13	965.2399	0.0002	0.745+/−0.04	0.802
16	6	10	17	5	12	965.3020	0.0005	0.150+/−0.03	0.162
8	2	6	8	1	8	965.3147	−0.0001	0.948+/−0.05	0.886
16	6	11	17	5	13	965.3216	0.0001	0.176+/−0.02	0.163
24	4	21	24	3	21	965.3278	−0.0004	0.332+/−0.01	0.357
13	3	11	13	2	11	965.4595	−0.0002	1.340+/−0.06	1.440
21	3	18	20	4	16	965.4698	−0.0003	0.808+/−0.04	0.756
20	2	18	19	3	16	970.4917	−0.0002	0.558+/−0.07	0.558
10	3	7	10	2	9	970.5300	0.0001	1.284+/−0.12	1.381
21	4	17	22	1	21	970.6355	0.0001	0.012+/−0.00	0.013
20	4	16	21	1	20	970.6686	−0.0003	0.016+/−0.00	0.015
8	1	7	7	0	7	970.7544	0.0000	1.709+/−0.14	1.597

The absolute intensities of ethylene lines were measured at room temperature. The pressure of gaseous C_2H_4 in the cell varied from ~0.3 to ~4 Torr. Figure 4 depicts the ethylene absorption spectra at different pressure obtained from processing of the corresponding transmission spectra. Line intensities were determined along with line positions and halfwidths. For this purpose, we fitted the C_2H_4 absorption spectrum using Voigt profile. The relative measurement error in absolute intensities was within 8%. The errors in determination of line strength were largely caused by the errors in determination of low pressure and intensity modulation of the laser signal due to interference and technical fluctuations.

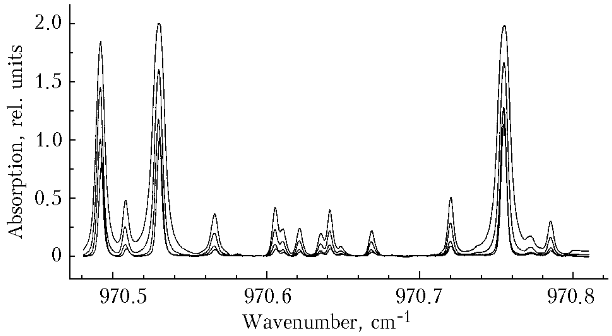

Fig. 4. Ethylene absorption coefficient measured at the pressure of 0.3, 0.75, 2, and 3 Torr.

Table 2 (column 4) presents the experimental data on the absolute intensities of transitions. Column 5 gives the line strengths calculated with the use of the refined dipole moment derivative with respect to the normal coordinate ($\delta\mu_\chi/\delta q_7 = 0.23 \pm 0.02$ D). In our calculation of line strengths, we used the rigid asymmetric top model, because the accuracy in determination of line strengths was insufficient to take into account the effects caused by the Coriolis resonance. Nevertheless, the obtained data agree well with similar data from the GEISA atlas of spectral lines.[2] The mean discrepancy is about 5%.

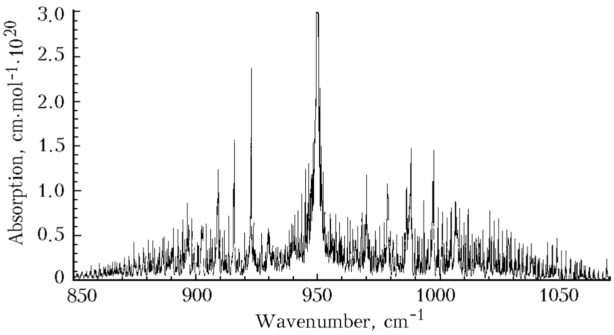

Fig. 5. Calculated ethylene absorption spectrum in the region of 9–12 μm.

Figure 5 shows the ethylene absorption spectrum in the region up to 12 μm as calculated based on the obtained data for the following parameters: $T = 296$ K, $P_{C_2H_4} = 2$ Torr, $P_{tot} = 750$ Torr.

Conclusion

This paper has presented analysis of rotational-vibrational lines of the ν_7 band of ethylene recorded with a tunable diode laser spectrometer. The absolute accuracy in determination of line positions was no less than 0.0003 cm^{-1}. The measured absolute intensities of 20 lines have allowed us to refine the derivative of the dipole moment with respect to the normal coordinate.

References

1. L.S. Rothman, C.P. Rinsland, A. Goldman, et al., J. Quant. Spectrosc. Radiat. Transfer **60**, No. 5, 665–710 (1998).
2. The GEISA Line Parameters Data Bank in 1984, Ann. Geophys. **4**, No. 2, 185–186 (1986).
3. O.K. Voitsekhovskaya, A.V. Rozina, and N.N. Trifonova, *Information System on High-Resolution Spectroscopy* (Nauka, Novosibirsk, 1988), 150 pp.
4. F.J.M. Harren, J. Reuss, E.J. Woltering, and D.D. Bicanic, Appl. Spectrosc. **44**, No. 8, 1360–1368 (1990).
5. W.L. Smith and I.M. Mills, J. Chem. Phys. **40**, 2095–2109 (1964).
6. Ch. Lambeau, A. Fayt, J.L. Duncan, et al., J. Mol. Spectrosc. **81**, 227–247 (1980).
7. D.L. Johansen, *Thesis* (University of Minnesota, 1973), 127 pp.
8. G.P. Montgomery, Jr, and J.C. Hill, J. Opt. Soc. Am. **65**, 579–585 (1975).
9. F. Herlemont, M. Lysryk, J. Lemaire, Ch. Lambeau, and A. Fayt, J. Mol. Spectrosc. **74**, 400–408 (1979).
10. Cauuet, A. Valentin, Ch. Lambeau, et al., J. Mol. Spectrosc. **139**, 191–214 (1990).
11. F. Herlemont, M. Lysryk, J. Lemaire, Ch. Lambeau, M. DeVleeschouwer, and A. Fayt, J. Mol. Spectrosc. **94**, 309–315 (1982).
12. E. Willemot, J. Mol. Spectrosc. **120**, 246–275 (1986).
13. Yu.V. Kosichkin, A.I. Kuznetsov, et al., Kvant. Elektron. **9**, No. 4, 882–885 (1982).
14. G. Guelachvili and K. Narahary Rao, *Handbook of Infrared Standards* (Academic Press, New York, 1986).
15. J.L. Duncan, D.C. McKean, and P.D. Mallinson, J. Mol. Spectrosc. **45**, 221–245 (1973).
16. J. Wathson, J. Chem. Phys. **46**, 1935–1949 (1967).